

Electric Field Forced Vibration of a Periodic Piezocomposite Plate
with Laminated Structure and
Reflection and Transmission of a Plane Wave at the Fluid-Composite Interface

Q. M. Zhang and Xuecang Geng

Materials Research Laboratory, The Pennsylvania State University
University Park, PA 16802

Abstract:

We address the problems of the vibration of a periodic piezo-composite plate (2-2 composite) under external electric fields and the reflection and transmission of a plane wave incident on the fluid-composite interface based on an analytical method developed recently, which takes into account explicitly the heterogeneous nature of the piezocomposites. It is shown that due to the finite thickness of the composite plate, a series of piezo-active modes at frequencies near and above the stop band edge mode frequency may be excited. It is also shown that as a result of the heterogeneous structure of the composite, the reflection coefficient from the fluid-composite interface is a complex number, which should have important implication on the design of quarter wave matching layer in composite transducers.

I. Introduction.

Piezoceramic polymer composites have been widely used in areas such as ultrasonic medical imaging and non-destructive evaluation and exhibit many attractive features in these applications in comparison with single phase piezoelectric materials.¹ Since as a diphasic material, the effective properties of a composite depend crucially on the properties of the constituents, the quantitative study of their properties is an interesting and important problem in order to optimize composite transducers for different applications. However, due to the fact that for ultrasonic applications, the aspect ratio of the composite unit cell, which is L/d for a composite with 2-2 connectivity as schematically drawn in figure 1, is not large (usually in the range between 2 and 6) and the acoustic wavelength is also comparable to the spatial period d , the usual averaging schemes such as those based on either the Reuss (isostress) model or Voigt (isostrain) model² in treating the elastic and electromechanical properties of a composite become inadequate. While finite element analysis (FEA) can provide some information on how the properties of the constituents affect the ultrasonic performance of a composite transducer under these conditions, it is quite time consuming if a systematic study is intended and to some extent, FEA is a computer experiment and, hence, does not provide a lot of physical insight into the problem investigated. Clearly, analytical models which take into account the heterogeneous structure of a composite and can bridge the gap between the earlier simple models on composite materials and FEA should be developed.

Recently, based on the method of partial wave expansion, a theoretical model was established for composites with a periodic laminate structure and finite aspect ratio L/d .^{3,4} For a periodic laminate composite plate as schematically drawn in figure 1, since the dimension in the x_2 -direction is much larger

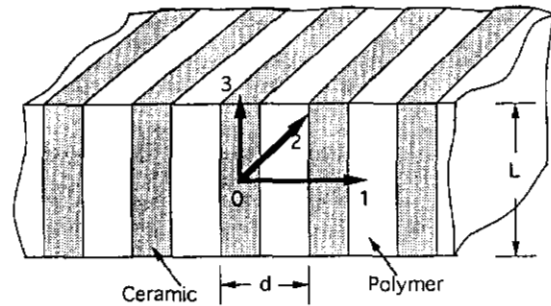


Figure 1. Schematic drawing of a periodic piezoceramic polymer composite plate. The poling direction of the piezoelectric ceramic plates is along the x_3 -direction. The width of ceramic plate is $v d$ and the width of polymer is $(1-v) d$, where v is the ceramic volume content in the composite.

than L and d , the problem can be treated as a two dimensional one. Here, the solution to a bounded composite plate is obtained by summation over the solutions of guided waves in unbounded plates.⁵ Unlike the earlier approach, the solutions to unbounded composite plates are obtained by solving the dynamic elastic equations in the ceramic phase and polymer phase separately and matching the two by the boundary conditions at the ceramic-polymer interface. Hence, the problem of averaging the properties of a composite in the x_1 -direction is avoided.

The guided wave solutions to the dynamic elastic equations in the unbounded ceramic plate are:

$$\begin{aligned} u_3^c &= \sum_{i=1}^3 R_i^c f_i^c \cos(h_i^c x_1) \exp(j \beta x_3) \\ u_1^c &= \sum_{i=1}^3 R_i^c g_i^c \sin(h_i^c x_1) \exp(j \beta x_3) \\ \Phi^c &= \sum_{i=1}^3 R_i^c t_i^c \cos(h_i^c x_1) \exp(j \beta x_3) \end{aligned} \quad (1)$$

where f_i^c , g_i^c , and t_i^c are factors depending on β and h_i , the wave vector components in the x_3 and x_1 directions, and $j = \sqrt{-1}$. Similar equations can be written for the polymer plate.^{3,4}

The superscripts c and p are introduced to denote the ceramic and polymer, respectively. In eq. (1), the symmetry conditions in the x_1 -direction for the piezoelectric active mode in a periodic composite plate are used, and for the sake of

simplicity, the time dependent term ($\exp(j\omega t)$), where ω is the angular frequency and t is time, is omitted. The boundary conditions of the stresses, elastic displacements, and the electric displacement and potential at the ceramic-polymer interface ($x_1 = vd/2$) yield six homogeneous linear equations which relate the six undetermined coefficients R_i^p and R_i^c . The condition for a nontrivial solution of homogeneous linear equations requires that the determinant of the coefficients vanishes, i.e.,

$$K = |\text{coefficients of } R_i| = 0 \quad (2)$$

where the coefficients of R_i are functions of the β , d , the angular frequency ω , the ceramic volume fraction v , and the material parameters of both the polymer and piezoceramic. Equation (3) yields the relationship between β and f , the dispersion curves. For each point on the dispersion curves, the relations among R_i^p and R_i^c can be determined from the homogeneous linear equations. Shown in figures 2(a) and 2(b) are the dispersion curves for composite plates with 15% and 44% ceramic content, respectively. The parameters used in the calculation are those of PZT-5H for the piezoceramic and Spurrs epoxy for the polymer phase, respectively.⁶ In addition, for $\beta=0$, the solutions in the ceramic and polymer plates which satisfy the boundary conditions at $x_1=vd/2$ are:

$$u_1^c = k_1 C \sin(h_{01}^c x_1), \quad u_1^p = k_2 C \sin(h_{01}^p (x_1 - \frac{d}{2})), \quad (3)$$

$$\Phi^c = \Phi^p = C x_3$$

where k_1 and k_2 are constants, $h_{01}^c = \sqrt{\frac{\rho^c}{c_{11}^c}} \omega$, $h_{01}^p = \sqrt{\frac{\rho^p}{c_{11}^p}} \omega$.

In this paper, two situations will be considered explicitly based on the results presented. The first one is a composite plate situated in air and subjected to an AC applied electric field where the electric impedance, resonant mode frequencies, and surface vibration profile will be calculated. The second one is the wave propagation in a fluid-composite system as schematically drawn in figure 3. From the reflection coefficients, the input acoustic impedance at the fluid-composite interface as a function of frequency can be evaluated.^{7,8} Clearly, the quantities evaluated here can be measured experimentally and are of great importance to the understanding of ultrasonic performance and optimum design of a composite transducer.

II. Forced vibration of a finite thickness composite plate.

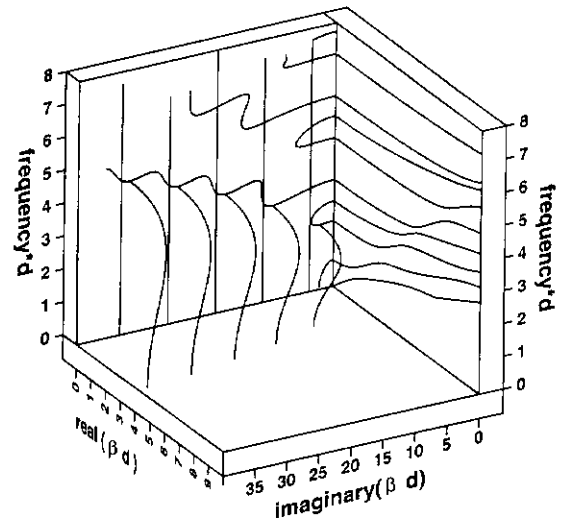
To treat a composite plate situated in air under an AC electric field, u_3 , u_1 , and ϕ are expanded in terms of the eigenfunctions in an unbounded system. For the ceramic plate:

$$u_3^c = \sum_{n=1}^m \sum_{i=1}^3 k_{ni}^c f_{ni}^c \cos(h_{ni}^c x_1) \sin(\beta_n x_3) A_n$$

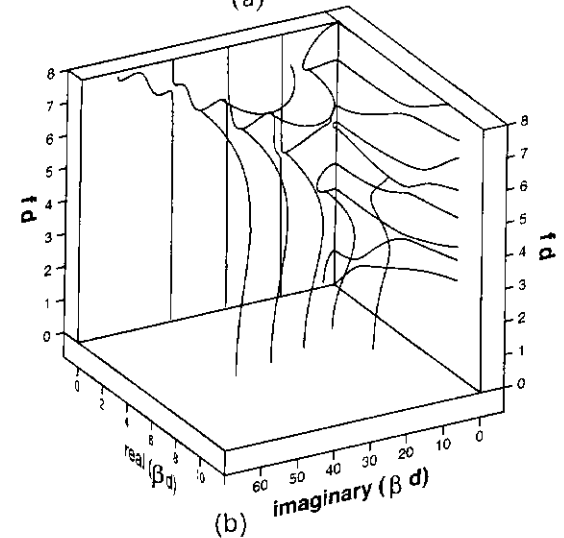
$$u_1^c = \sum_{n=1}^m \sum_{i=1}^3 k_{ni}^c g_{ni}^c \sin(h_{ni}^c x_1) \cos(\beta_n x_3) A_n + C k_1 \sin(h_{01}^c x_1)$$

$$\Phi^c = \sum_{n=1}^m \sum_{i=1}^3 k_{ni}^c t_{ni}^c \cos(h_{ni}^c x_1) \sin(\beta_n x_3) A_n + C x_3 \quad (4)$$

A similar solution can be written for the polymer plate. In eq. (4), k_{ni} , f_{ni} , g_{ni} , and t_{ni} are constants. A_n and C are determined by the boundary conditions which are traction free and $\phi = \pm \phi_0/2$ at $x_3 = \pm L/2$. With a finite number of eigenfunctions in the expansion, the boundary conditions at $x_3 = \pm L/2$ cannot be satisfied at all x_1 . The number of the



(a)



(b)

Figure 2. Dispersion curves for a composite made of PZT-5H ceramic and Spurrs Epoxy with 15% ($v=0.15$) (the top figure) and 44% ceramic volume content ($v=0.44$) (the bottom figure).

eigenfunctions, m , required, hence, is determined by the accuracy needed for the solution. For the problem treated here, we found that it is adequate to use eight eigenmodes in the expansion. In the frequency range studied ($fd < 2$ in figure 2), there are two branches with real β and other branches having either imaginary or complex β , which corresponds the modes confined at the boundary $x_3 = \pm L/2$ (surface modes).

The coefficients A_n and C in eqs. (4) are determined by the variational technique.⁵ Based on u_3 , u_1 , and ϕ thus determined, all the properties related to the vibration problem of a composite plate can be evaluated. Shown in figure 4(a) is the electric impedance spectrum for a composite plate with 44% ceramic content made of PZT-5H piezoceramic and Spurrs epoxy with $L/d = 4.49$. The electric impedance Z_e is calculated

from the relation $Z_e = \phi_0/I$ where $I = j \omega \int D_3 dx_1$. The

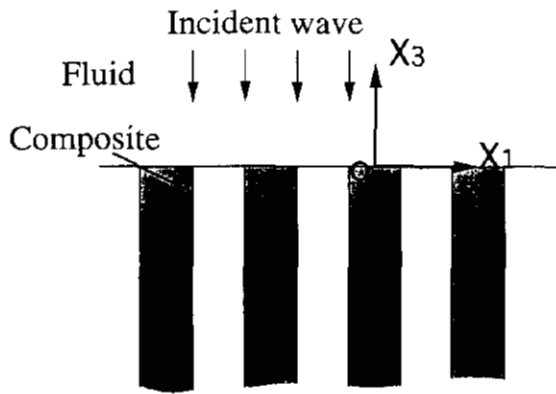


Figure 3. Schematic drawing of a plane wave incident normally at the fluid-2-2 composite interface, where the fluid occupies the upper half space and the piezocomposite the lower half space.

integration is over one unit cell for D_3 at $x_3 = L/2$, where D_3 is the electric displacement vector component along the x_3 -direction ($D_3 = e_{33}u_{3,3} + e_{31}u_{1,1} - \epsilon_{33}\phi_{,3}$). For the comparison, the electric impedance measured experimentally from the same composite is shown in figure 4(b) and clearly the theoretical impedance curve reproduces the experimental data quite well. One interesting feature revealed in the figures is that in a composite plate, in addition to the thickness resonance mode, there exist other modes due to the periodic nature of the composite and coupling between the two phases. In figure 5, we display the distributions of u_3 at each mode. Apparently, f_{L1} is the fundamental thickness resonance and f_{t1} is the stop band edge resonance as revealed by the fact that the ceramic and polymer vibrate 180° out of phase at this mode, which has been predicted in the earlier theoretical work.⁹ The frequency position and the distribution of u_3 along the x_3 -axis indicate that f_{L3} is third harmonic of the thickness mode. However, the appearance of f_{t2} is not expected from the earlier theoretical works. By examining the equations of the boundary conditions at $x_3 = \pm L/2$, it can be deduced that a resonance will occur whenever $\beta = (1+2n)\pi/L$, i.e., $\cos(\beta L/2) = 0$. From the dispersion curves of real β , as shown in figure 4(c), it is clear that the fundamental thickness resonance and the stop band edge resonance occur at $\beta = \pi/L$ (f_{L1} and f_{t1}). Similarly, when $\beta = 3\pi/L$, the third harmonic of the thickness mode will occur at f_{L3} . In addition, a mode f_{t2} will also show up at the branch 1 which is at a frequency near and above f_{t1} . By the same argument, it would be expected that f_{t3} , f_{t4} , etc. may also be observed, depending on the electromechanical coupling factors of these modes. It can be shown that the effective coupling factor for these modes decreases rapidly for the higher order modes. These features have been observed experimentally and the results here provide a clear physical picture for the experimental observation.

For a composite plate to work effectively as an electromechanical transduction material, it is required that the ceramic and polymer vibrate in phase with nearly the same amplitude in the x_3 -direction. The evolution of the vibration pattern in the two plates with frequency and the aspect ratio L/d of a composite plate is studied here. Shown in figure 6(a) is the change of the ratio u_{3p}/u_{3c} at $x_3 = L/2$ (at the surface of the composite plate), where u_{3p} and u_{3c} are u_3 at the centers of the

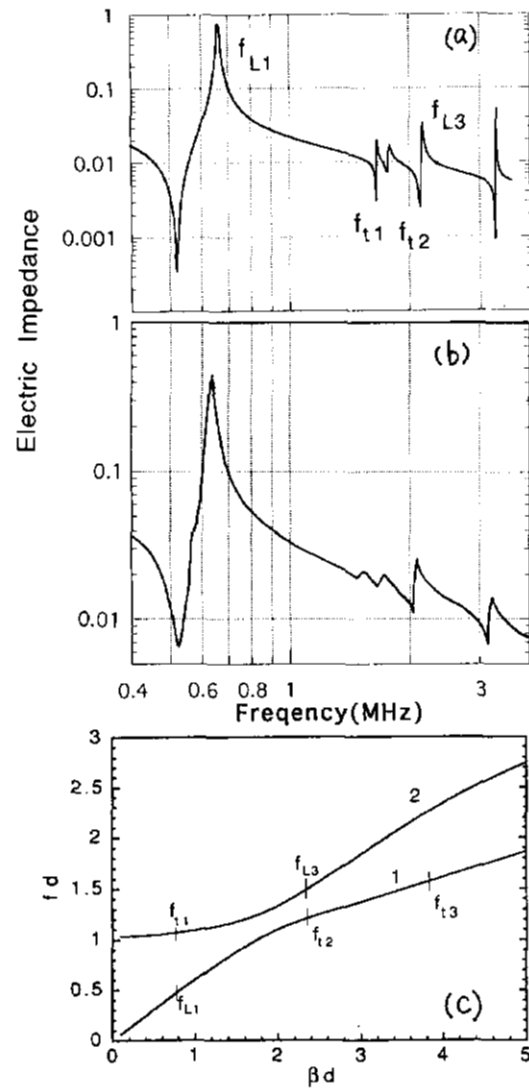


Figure 4. (a) The impedance spectrum for $\nu = 0.44$ composite plate of $L/d = 4.49$. (b) Experimental results for a 2-2 composite with $\nu=0.44$ and $L/d = 4.49$ which can be compared with figure (a), the theoretical result. (c) The dispersion curves for $\nu=0.44$ composite which show the positions of the possible resonant modes in a finite thickness plate. f_{L1} and f_{t1} occur at $\beta=\pi/L$, f_{L3} and f_{t2} occur at $\beta=3\pi/L$. Hence, f_{t3} will occur at $\beta=5\pi/L$, etc. Whether these high order modes f_{t2} , f_{t3} , etc. be observed experimentally depends on the electromechanical coupling factors for these modes.

polymer phase ($x_1=d/2$) and the ceramic ($x_1=0$) respectively, with frequency for the composite plate of $L/d = 4$. At frequencies far below any resonance mode, u_{3p}/u_{3c} is always less than one. As L/d increases, this ratio increases and approaches one. These are consistent with the results of the earlier theoretical model developed.¹⁰ As frequency increases towards the thickness resonance, the ratio u_{3p}/u_{3c} also increases towards one. At a frequency f_1 which is near f_s of the thickness mode, where f_s is the series resonant frequency, $u_{3p}/u_{3c}=1$. This is true as long as $f_{L1} < f_{t1}$. This ratio will

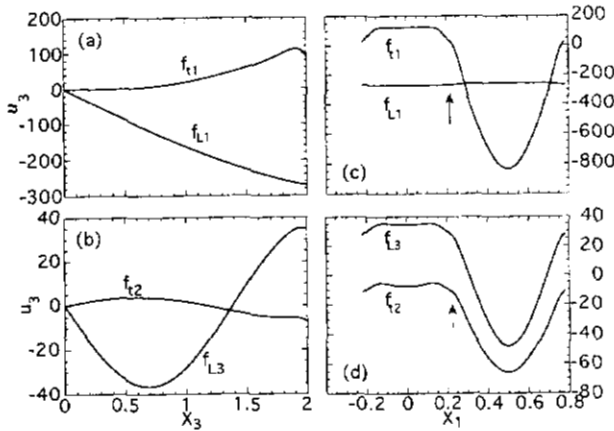


Figure 5. The distributions of u_3 for a composite plate of $\nu=0.44$ and $L=4$ ($d=1$) at f_{L1} , f_{11} , f_{L3} , and f_{12} . (a) and (b) u_3 at $x_1=0$ (at the center of ceramic plate) as a function of x_3 where $x_3=0$ is at the center and $x_3=2$ is at the surface of the composite plate. (c) and (d) u_3 at the surface of the composite plate as a function of x_1 . The arrows indicate the position of the interface between the ceramic and polymer. At f_{11} and f_{L3} , the ceramic and polymer vibrate out of phase with each other, while at f_{L1} and f_{12} , the two vibrate in phase.

surpass one as the frequency is further increased. In figure 6(b), the change of f_1/f_s vs. the aspect ratio L/d is presented. Clearly, f_1/f_s is near but larger than one except for composite plates with small aspect ratio. Hence, the aspect ratio L/d does not have a significant effect on the ratio of u_{3p}/u_{3c} at frequencies very near f_s of the thickness mode, where u_{3p}/u_{3c} is always near one. However, it will affect the bandwidth in

which u_{3p}/u_{3c} is near one. For example, the bandwidth $\frac{\Delta f}{f_1}$ in which $0.9 < u_{3p}/u_{3c} < 1.1$ increases as the aspect ratio L/d increases, which is shown in figure 6(b). In the practical design of a composite transducer, the aspect ratio L/d required, hence, will be determined by the operation bandwidth needed.

III. Reflection and transmission of a plane wave at fluid-composite interface

We now turn to the problem of the reflection and transmission of a plane wave normally incident at the fluid-composition boundary as depicted in figure 3, where the fluid occupies the upper half space ($z > 0$) and the composite the lower half space ($z < 0$) and a plane wave with wave vector β_0^f incident normally at the boundary. The solutions to the wave equation in the fluid phase ($z > 0$) are plane wave solutions and to satisfy the boundary conditions at the fluid-composite interface, u_1^f and u_3^f are expanded in terms of these plane wave solutions:

$$u_1^f = \sum_{n=1}^J k_{xn} R_n \sin(k_{xn} x_1) \exp(j\beta_n^f x_3)$$

$$u_3^f = \beta_0^f \exp(-j\beta_0^f x_3) - \sum_{n=0}^J \beta_n^f R_n \cos(k_{xn} x_1) \exp(j\beta_n^f x_3) \quad (5)$$

where $k_{xn} = \frac{2n\pi}{d}$ and $\beta_n^f = \sqrt{(\beta_0^f)^2 - (k_{xn})^2}$ are the wave vector components along x_1 and x_3 - directions, respectively. In the frequency range where an ultrasonic piezocomposite transducer is operated, β_n^f is imaginary except $n=0$. The reflection

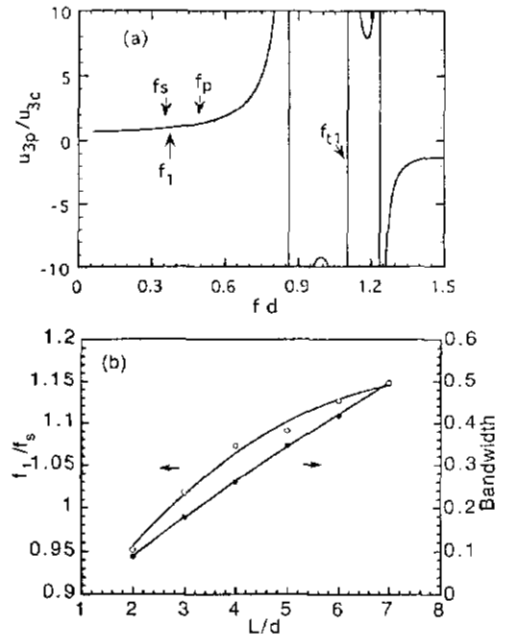


Figure 6. (a) The ratio of u_{3p}/u_{3c} vs. frequency (fd) for the composite plate of $\nu=0.44$ and $L/d=4$. (b) The frequency ratio f_1/f_s and the bandwidth $\Delta f/f_1$, where Δf is defined as the frequency range in which $0.9 < u_{3p}/u_{3c} < 1.1$ as a function of the aspect ratio L/d for a composite plate with $\nu=0.44$.

coefficient, hence, is $-R_0$ which can be measured experimentally.

The solutions in the composite region are:

$$u_1^c = \sum_{n=1}^m \sum_{i=1}^3 jbc_{ni} \sin(h_{ni}^c x_1) \exp(-j\beta_n x_3) A_n$$

$$u_3^c = \sum_{n=1}^m \sum_{i=1}^3 ac_{ni} \cos(h_{ni}^c x_1) \exp(-j\beta_n x_3) A_n \quad (6)$$

$$\Phi^c = \sum_{n=1}^m \sum_{i=1}^3 cc_{ni} \cos(h_{ni}^c x_1) \exp(-j\beta_n x_3) A_n$$

for the ceramic plate and similar equations can be written for the polymer region. In the above equations, bc_{ni} , ac_{ni} and cc_{ni} are proportional constants, A_n and R_n are determined by the boundary conditions at the fluid-composite interface $x_3=0$. The variational technique is used to determine these coefficients. The number of terms in the expansions (J in eqs. (5) and m in eqs. (6)) is determined by the accuracy desired. In the calculation carried out here, $J=5$ and $m=8$ are used.

Shown in figure 7 is the reflection coefficient R for the composites made of PZT-5H piezoceramic and Spurr's epoxy with 15% and 44% ceramic content, respectively, where parameters of water are used for the fluid medium. The large change in the reflection coefficient at fd near 1 for 44% (fd near 0.8 for 15%) is due to the lateral mode in the composites where the ceramic and polymer vibrate out of phase. Evidently, R is not a pure real number but has an imaginary component, reflecting the heterogeneity nature of the composites.⁸ Only at low frequency region, does the imaginary part become zero. This is fundamentally different from single phase materials. From the classical wave propagation in elastic medium problem, the input acoustic impedance of the composite Z_{in} at

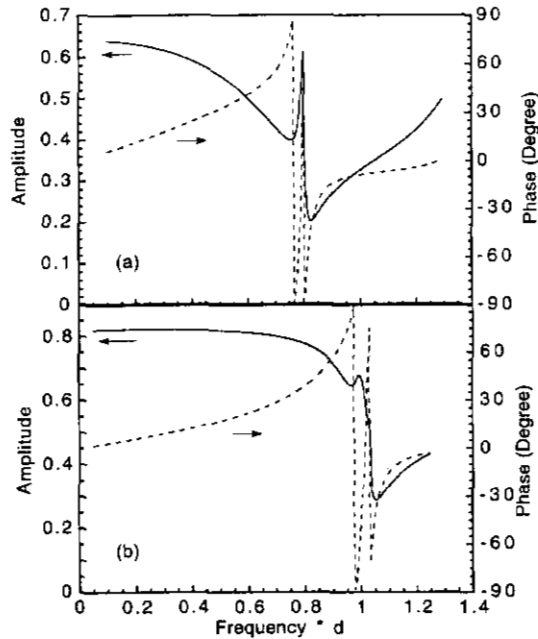


Figure 7. The reflection coefficient R from the water piezocomposite interface for a plane wave normally incident at the interface for (a) the ceramic volume content v in the composite is 15%; (b) the ceramic volume content v in the composite is 44%. The polymer and piezoceramic used in the composites are Spurr's epoxy and PZT-5H. The solid lines are the amplitude and dashed lines are the phase angle of R . The absolute phase angle is that displayed plus 180° . The non-zero phase angle for the reflection coefficient at the fluid-composite interface will affect the choice of the thickness of the matching layer for a composite transducer.

the interface can be calculated from the relation:

$$R = \frac{Z_f - Z_{in}}{Z_f + Z_{in}} \quad (7)$$

where Z_f is the characteristic acoustic impedance of the fluid.^{7,8} Since Z_f is assumed independent of frequency and real for water, Z_{in} exhibits a frequency dependent behavior and has a non-zero phase angle as shown in figure 8. Again, only at low frequencies, Z_{in} is equal to that calculated from the averaged density of the composites times the effective longitudinal velocity.¹¹ The strong frequency dependence of the acoustic impedance for piezocomposites was also observed in an earlier experiment¹² and further experiment will be carried out to verify the analytical results.

Another standard method for calculating the input acoustic impedance of the composite at $x_3=0$ is from the relationship between the stress and the sound velocity at the interface.^{7,8} For a composite considered here, both the stress and velocity are functions of x_1 and to calculate Z_{in} , we assume that the averaged values can be used:

$$Z_{in} = -\frac{\bar{T}_3}{\bar{v}_3} \quad (8)$$

where \bar{T}_3 and \bar{v}_3 are the averaged stress component and averaged velocity (over one unit cell) in the x_3 -direction evaluated at $x_3=0$. The results are also shown in figure 8 (dashed lines). As seen from the figure, the two results agree with each other quite well.

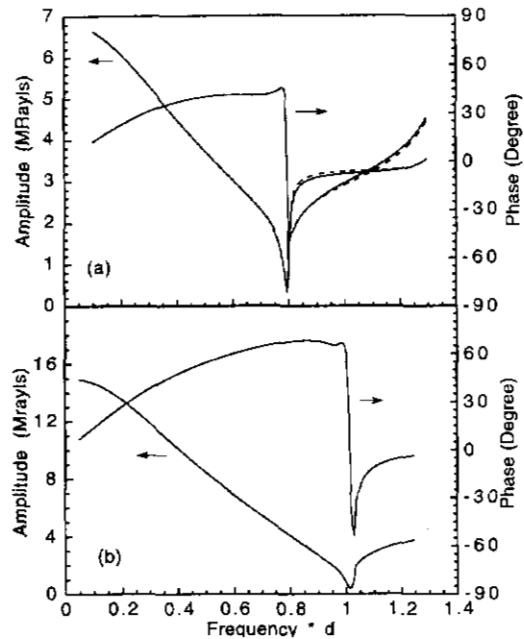


Figure 8. The input acoustic impedance for the composite calculated from the reflection coefficient R (solid lines) and from the stress-sound velocity relationship (dashed lines) for (a) composite with 15% ceramic content and (b) composite with 44% ceramic content. Unlike single phase materials, the input acoustic impedance for a composite is a complex. Only at low frequencies, the acoustic impedance is equal to those calculated from the effective medium theory.

IV. Summary.

Based on the analytical method developed recently, we treated quantitatively the vibration problem of a finite thickness piezoceramic polymer composite under an external AC field and wave propagation and input acoustic impedance at a fluid piezocomposite interface. The results reveal many interesting and important features related to the resonant modes and vibration profiles in a piezocomposite plate, and the characteristics of the reflection and transmission of a plane wave and input acoustic impedance at the fluid composite interface, which should have important implications to the design of the matching layer in a composite transducer. The results are in good agreement with existing experimental data.

V. Acknowledgment.

This work was supported by the Office of Naval Research through the Grant No. N00012-93-1-0304.

References:

1. W. A. Smith, Proc. 1990 IEEE ISAF7, 145 (1990).
2. S. Less and C. L. Davidson, IEEE Trans. on Sonics and Ultrasonics, **SU-24**, 222 (1977).
3. X. Geng and Q. M. Zhang, Appl. Phys. Lett. **67**, (1995).
4. Y. Shui, X. Geng, and Q. M. Zhang, IEEE Trans. UFFC **42**, 766 (1995).
5. H. F. Tiersten, "Linear Piezoelectric Plate Vibrations" (Plenum, New York, 1969).
6. PZT-5H is the trade-mark of Morgan Matroc Inc. Spurr's epoxy is the trade-mark of Polysciences, Inc. The parameters used are: PZT-5H: $e_{33} = 23.09$ C/m², $e_{31} = -6.603$, $e_{15} =$

17.0, $c_{11} = 12.72 \times 10^{10}$ N/m², $c_{44} = 2.3 \times 10^{10}$, $c_{33} = 11.74 \times 10^{10}$, $c_{13} = 8.47 \times 10^{10}$, $\epsilon_{11}/\epsilon_0 = 1700$, $\epsilon_{33}/\epsilon_0 = 1470$, $\rho = 7500$ kg/m³. Spurr's epoxy: $c_{11} = 5.4 \times 10^9$ N/m², $c_{44} = 1.3 \times 10^9$, $\rho = 1100$ kg/m³.

7. B. A. Auld, "Acoustic Fields and Waves in Solid" (John Wiley & Sons, N.Y., 1973).

8. L. M. Brekhovskikh, "Waves in Layered Media" (Academic Press, N. Y. 1980).

9. Y. Wang, E. Schmidt, and B. A. Auld, Proc. IEEE Ultrasonic Symp. (1986) p. 685.

10. Q. M. Zhang, W. Cao, J. Zhao, L. E. Cross, IEEE Trans. UFFC 41, 556 (1994).

11. W. A. Smith and B. Auld, IEEE Trans. UFFC 38, 40 (1988).

12. T. R. Gururaja, Ph. D. Thesis, Penn State University (1984).